INSIGHT TO THE MICROSTRUCTURE CHARACTERIZATION OF A HP AUSTENITIC HEAT RESISTANT STEEL AFTER LONG-TERM SERVICE EXPOSURE

Mahyar Mohammadnezhad[1)], Vahid Javaheri[2)], Morteza Shamanian[1)], Shahram Rizaneh[1)], Jerzy A. Szpunar[3)]*

[1)] *Department of Materials Engineering, Isfahan University of Technology, Isfahan 84156-83111, Iran*

[2)] *Department of Material Engineering and Production Technology, University of Oulu, Oulu 90570, Finland*

[3)] *Department of Mechanical Engineering, University of Saskatchewan, Saskatoon, SK, S7N5A9, Canada*

Received: 30.10.2018
Accepted: 07.11.2018

[*]*Corresponding author: e-mail: m.mohammadnezhad@ma.iut.ac.ir, Department of Materials Engineering, Isfahan University of Technology, Isfahan 84156-83111, Iran*

Abstract

Heat-resistant steels of HP series (Fe-25Cr-35Ni) are used in high temperature structural applications. Their composition include Nb as strong carbide former. Electron Backscatter Diffraction (EBSD) investigations revealed that, in the as-cast condition, alloys exhibit austenitic matrix with intergranular primary carbides such as MC, $M_{23}C_6$ and/or M_7C_3. During exposure at a high temperature, phase transformations occurred: chromium carbides of M_7C_3 type transform into the more stable $M_{23}C_6$ type, intergranular $M_{23}C_6$ carbides precipitate, and Lave phase due to increase of Niobium activity with temperature increase, as thermodynamic simulation confirmed. Therefore, combination of EBSD-EDS technique with thermodynamic calculation is one of the novel and most accurate method to investigation of phase transformation, as the precipitations are identified on the basis of their crystal structure, chemical composition and their thermodynamic features.

Keywords: Austenitic heat resistant steels, chromium carbide, Laves phase, EBSD, thermodynamic simulation

1 Introduction

Heat resistant cast steels are widely used in various high temperature industrial applications thanks to their excellent creep strength, oxidation and abrasion resistance at elevated temperatures. The HP (Fe-25Cr-35Ni) steel which is one of the most important austenitic heat resistant alloy that has a combination of creep strength and resistance to oxidizing and carburizing atmospheres at service temperature around 1000°C [1].

As regards the austenitic microstructure, HP heat resistant steel type is being developed for different applications vary from pyrolysis in petrochemical industries to reformer furnaces in steel making factories. These grades of steel have replaced the traditional nickel based super alloys with a substantial reduction of cost and have equivalent properties under conditions of creep, with excellent resistances to high temperature oxidation and metal dusting [2].

DOI 10.12776/ams.v24i4.1160 p-ISSN 1335-1532
e-ISSN 1338-1156

Although this alloy steel castings are designed for use at elevated temperatures, metallurgical degradation, aging and phase transformations can occur after extended service exposure above 800 °C, potentially resulting in embrittlement. The typical microstructure of as-cast alloy is an austenite matrix with intergranular eutectic-like primary chromium-rich carbides (M_7C_3 and/or $M_{23}C_6$ types) and niobium carbides (MC type) [3-4]. Long-term service at high temperature of heat-resistant steels can bring about decomposition of austenite and forming of carbides and intermetallic compounds such as sigma, chi, Laves, and epsilon phases [5]. In addition, all the primary chromium carbides eventually transform into $M_{23}C_6$; intragranular secondary $M_{23}C_6$ carbides also precipitate [6]. These changes usually result in higher strength but also causes a loss of ductility at ambient temperature, leading to potential repair problems during shutdown, so it is important to be able to fully characterize the microstructure of both as-cast and aged alloys [1, 6].

Although a number of studies, e.g. [1-9], have been conducted subsequently to evaluate of phase changes during service and the influence of these changes on the failure mechanisms on 25Cr-35Ni-type heat-resistant cast steel, there is still a lacking of detailed investigations on the microstructural evolution after long-term service by using EBSD, such as phase orientation, and phase map.

In this paper, the microstructural evolution of two HP steels in as cast condition and after long time service exposure have been characterized by means of EBSD techniques. Our objective, in this work, is to address the phase transformation during aging (service condition) in high temperature in depth.

2 Experimental Procedures

In this work, two alloys of a HP heat resistant steel were studied: an as-cast alloy (A), and an ex-service alloy (X). The alloy B has stayed in service at approximately 900°C under a stress of 12 MPa for more than 10 years. Average chemical composition is presented in **Table 1**.

Table 1 Chemical composition of the sample in the as-cast condition (wt.%)

Element	C	Si	Mn	Cr	Ni	Mo	Nb	Fe
Amount	0.45	1.03	1.56	24.56	35.06	0.13	1.22	Bal.

The materials examined were pieces with the 10×20×40 mm dimensions. Microstructural investigation was carried out using a Hitachi SU6600 Scanning Electron Microscope (SEM) equipped with an Energy Dispersive X-ray Spectroscope unit (EDS) and an Electron Backscatter Diffraction (EBSD). The diamond polished samples were subsequently polished with 50 nm colloidal silica slurry for 6 h using Vibro Met 2 Vibratory polisher and etched in Marble's reagent. For obtaining orientation maps a voltage of 20 kV, working distance of 15 mm, and a step size of 50 nm were used. The HKL CHANNEL5 software was used to perform EBSD analysis and post-processing. In addition, thermodynamic simulation of the phases present in the HP alloy was performed with Thermo-Calc software V.2016b.

3 Result and Discussion

Fig. 1 illustrates the SEM microstructure of the as-cast condition (Alloy A) in two different magnifications; It has been clearly observed that microstructure consists of an austenitic matrix

DOI 10.12776/ams.v24i4.1160 p-ISSN 1335-1532
e-ISSN 1338-1156

(almost 87% relative area fraction) and a continuous network of primary precipitation (around 13%), located at the boundaries of grains and dendrites. The typical microstructure of HP alloys is an austenite matrix with intergranular eutectic-like primary chromium carbides with the stoichiometric composition of M_7C_3 and/or, $M_{23}C_6$ and MC type of niobium carbides [3, 8].

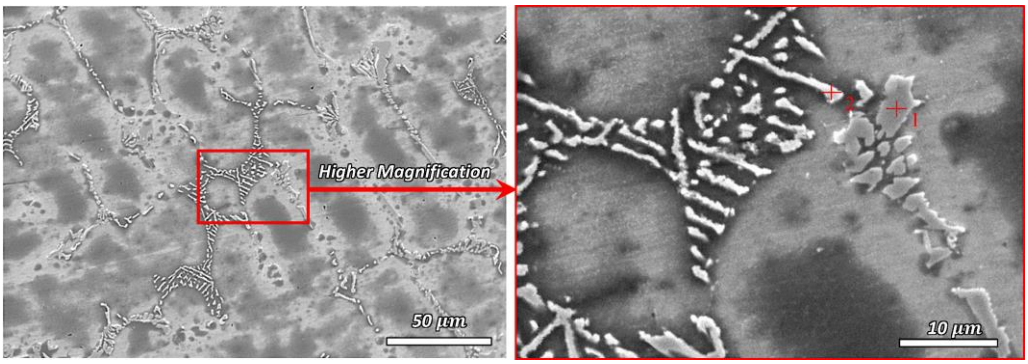

Fig. 1 SEM microstructure of the as-cast condition in two different magnifications

EDS analysis results, given in **Fig. 2**, reveal the precipitations could be identified as different type of carbides. Precipitates in most dark regions correspond to Cr-rich carbides (Point 1) whereas light contrast correspond to Nb-rich carbides (Point 2), as Nb has a much greater atomic weight than Cr.

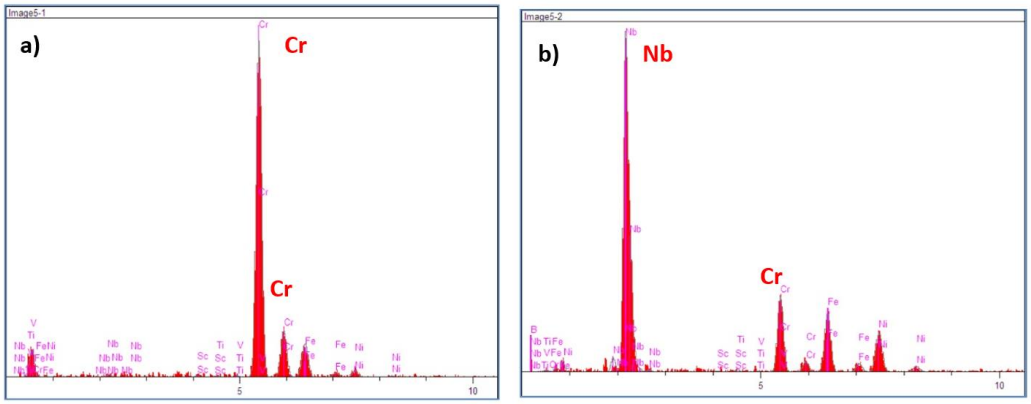

Fig. 2 EDS analysis results at two locations of alloy A, a) Point 1 and, b) Point 2

The SEM micrograph of the long-term (around 10 years) serviced sample (Alloy X) is presented in **Fig. 3**. The microstructure has significantly changed during the aging where the secondary precipitation decorates the austenitic matrix and is clearly defined at higher magnification. The secondary carbides strikingly increased and slightly grew in the matrix. The secondary carbides (mostly $M_{23}C_6$) precipitate inside the grains, due to the high solute supersaturation resulting from the casting process. In addition, primary carbides also coalesced and coarsened to form continuous films along grain boundaries.

DOI 10.12776/ams.v24i4.1160 p-ISSN 1335-1532
e-ISSN 1338-1156

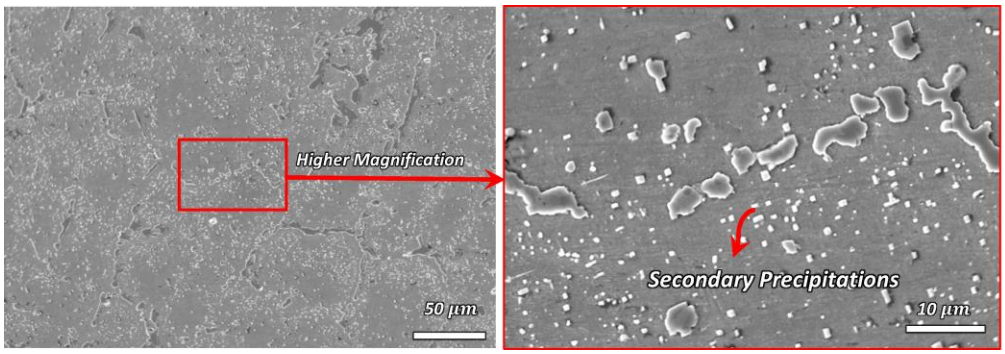

Fig. 3 SEM microstructure of the ex-serviced sample in two magnifications

Backscattered imaging contrast and/or EDS analysis can be used to make a difference between chromium carbides, MC carbides, and some other phases like G, Z and Laves phases, but they cannot differentiate $M_{23}C_6$ from M_7C_3 and M_6C due to low atomic number of carbon which causes difficulties to have a precise distinguish between those carbides. Therefore, a combination of EDS and EBSD would be an excellent tool to identify the various precipitates in the studied samples.

Fig. 4 illustrates EBSD IPF color map image of precipitates for the sample A and X. In the as cast condition, crystallographic orientation of all identified precipitates, as a network of primary carbide, in variety of colors is presented where M_7C_3 carbides have an orthorhombic structure with lattice parameter a = 4.49 Å, b = 6.93 Å and c = 12.02 Å, $M_{23}C_6$ carbides have a FCC structure with a lattice parameter a = 10.64 Å, M_6C carbides and MC have also a FCC structure with a lattice parameter a = 10.95 Å and a = 4.43 Å, respectively.

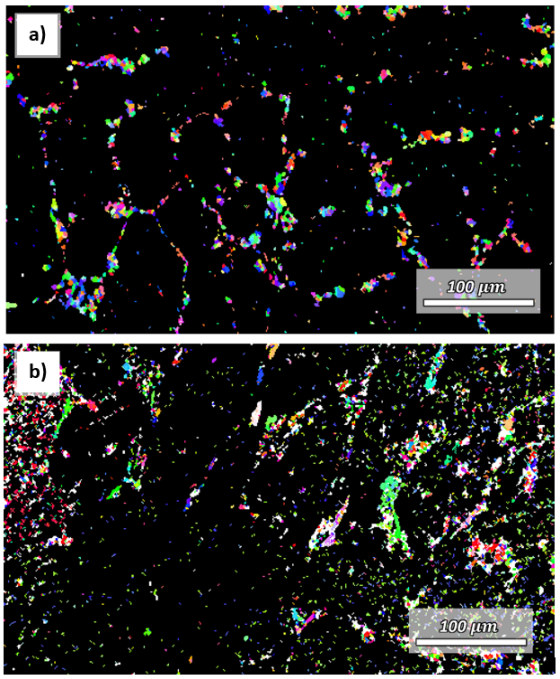

Fig. 4 IPF (Inverse Pole Figures) color map of a) Alloy A and b) Alloy X

DOI 10.12776/ams.v24i4.1160
p-ISSN 1335-1532
e-ISSN 1338-1156

Moreover, **Fig. 5** shows the EBSD phase color in the as cast (A) and after aging (X) condition. In the as-cast condition, three types of carbides can be detected as primary carbide: Cr_7C_3 and Cr_3C as chromium carbides and NbC as niobium carbide [9]. J. Liu et al. [3] reported that M_7C_3 carbides were clearly identified only in the as-cast sample but not in the aged and/or in the serviced sample, they suggested that the M_7C_3 carbides formed during the solidification and transformed into other phases after aging, this phenomenon also can be seen in **Fig. 5(b)**. It has been obvious that integrated EBSD and EDS technique helps to a very accurate phase identification. Indeed, the EDS spectrum along with diffraction pattern of each phase which are used to find all of matching phases and distinguishing the different type of chromium carbides that not possible to identify with other common methods. These results were also in agreement with Thermodynamic Scheil calculation results which could be considered to represent the sample microstructure constituents during solidification or in the as-cast condition, see **Fig. 6**. As observed, primary eutectic carbides are, thermodynamically, in nonequilibrium state, since they are formed due to carbon and chromium segregation to the dendritic cell boundaries. At elevated temperatures, these eutectic carbides are prone to the interaction with the FCC matrix towards equilibrium state. It has been also found that NbC forms at temperature higher than the temperature for $Cr_{23}C_6$ formation, it means that a significant amount of the total carbon is consumes by Nb before formation of $Cr_{23}C_6$. It could be the reason why of a very low amount of this type of chromium carbide in the as-cast condition [6].

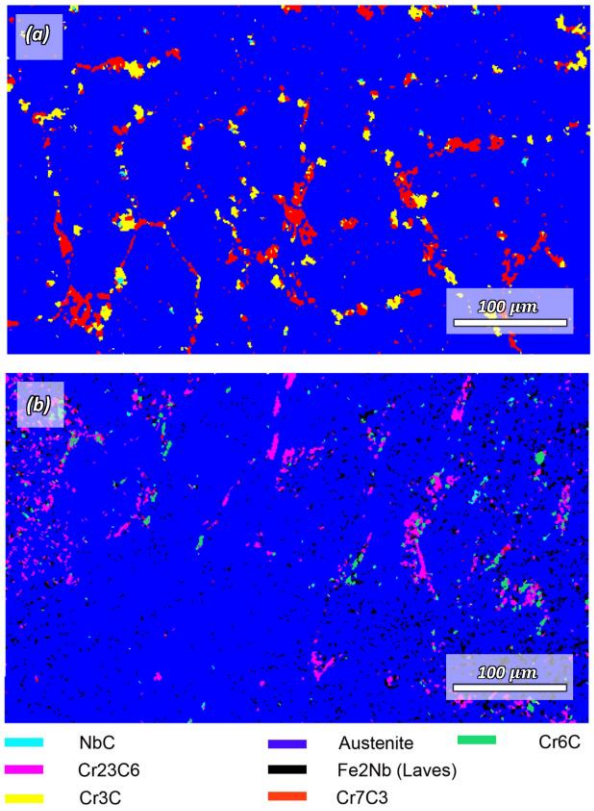

Fig. 5 EBSD phase color map of a) Alloy A and b) Alloy X

DOI 10.12776/ams.v24i4.1160 p-ISSN 1335-1532
e-ISSN 1338-1156

As the Cr_7C_3 carbide has an orthorhombic crystal lattice and is instable at high temperatures; it, therefore, transforms to $Cr_{23}C_6$ according to the following reaction:

$$2M_7C_3 + 9M = M_{23}C_6 \quad (1.)$$

where M is Cr combined with Fe [10]
In addition, under high temperature and time conditions, $Cr_{23}C_6$ partially transforms to Cr_6C according to the following reaction [10]:

$$M_{23}C_6 + 13M = 6M_6C \quad (2.)$$

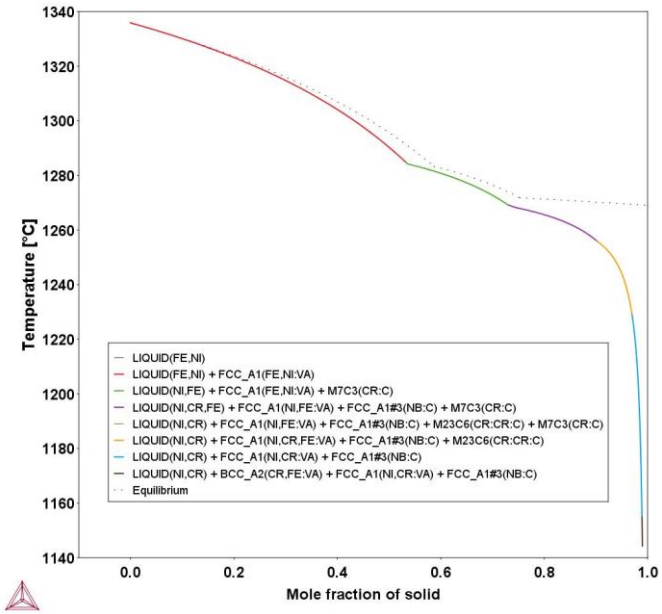

Fig. 6 Scheil calculation results for HP alloy with Thermo-Calc

In the sample X (**Fig. 5(b)**), due to service temperature many fine secondary $Cr_{23}C_6$ and Cr_6C carbides have been observed. As expected, the aging treatment resulted in considerable secondary or interdendritic carbides precipitation. Moreover, the coarsening of primary $Cr_{23}C_6$ carbide and agglomeration of secondary $Cr_{23}C_6$ carbide have been obviously occurred in the sample. Additionally, niobium carbide particles are detected where it could neither be identified by XRD due to its small amount nor by the TEM possibly due to their fall-off during electro polishing for preparing TEM foils. It can clearly see from the phase map that NbC particle being stable at the age temperature. The phase identification and image analysis data were schematically plotted in **Fig. 7** to illustrate the microstructure evolution during service exposure. It shows that almost all of the Cr_7C_3 in the as-cast condition appeared to be replaced by $Cr_{23}C_6$ and/or Cr_6C [11]. Besides, a small quantity of M_6C carbide formed bordering to $M_{23}C_6$. Some literatures [3, 12–14] also reported that M_6C carbide transformed from $M_{23}C_6$ kept twin OR with $M_{23}C_6$ /austenite, but M_6C carbide directly precipitated from the austenite kept a cube–cube OR with $M_{23}C_6$ /austenite. It may be explained that the 3 to 1 relation between $M_{23}C_6$ and austenite in lattice parameter, while the nearly 1 to 1 relation between M_6C and $M_{23}C_6$ have led to the twin

DOI 10.12776/ams.v24i4.1160 p-ISSN 1335-1532
e-ISSN 1338-1156

OR between the two phases. These two types of carbides present similar morphology with fine particle, and they are not easy to be distinguished using OM or SEM. In the other word, the remarkable microstructural evolution of the heat-resistant samples is attributed to their chemical composition and service condition. As the aging time and/or service time were prolonged, the precipitated carbide markedly increased, but their size hardly increased.

Moreover, 10 years of aging at 900◦C lead to the nucleation of fine intermetallic Fe_2Nb (Laves) phase, evenly dispersed needle-shaped precipitates in the size range of 3 μm and below throughout the austenitic matrix (**Figs. 5(b), 6**) and the grain boundaries. Laves phase is an intermetallic component of iron and other metallic elements like Nb, Mo and Ti. It has a hexagonal unit cell which necessitates close atomic size of its constituent elements. From the literature [15], Nb is known to be the most potent Laves phase former and its strong effect can be enhanced by combining it with Si [16].

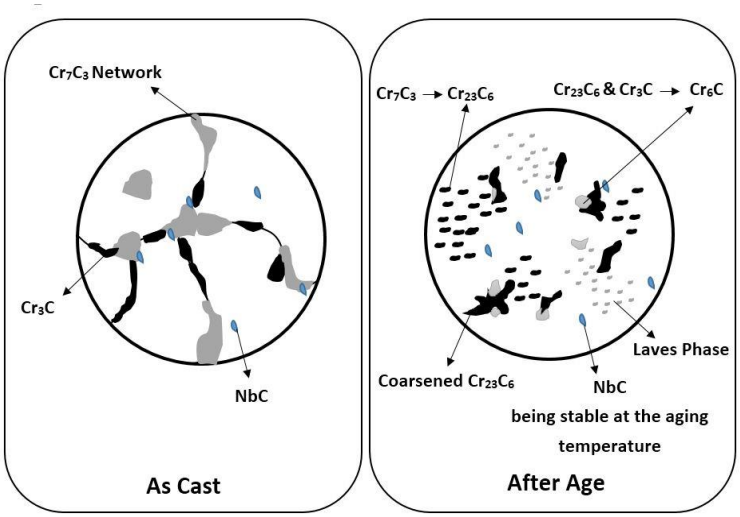

Fig. 7 Schematic illustration of phase transformation during aging in HP alloy

Thermodynamic calculation using Thermo-Calc software also confirmed the stability of NbC and increase of niobium activity as temperature increases which indicate to the possibility of Laves formation (**Fig. 8(a)**). Moreover, there is also coincidence of an increase in amount of $Cr_{23}C_6$ as amount of Cr_7C_3 decreases (**Fig. 8(b)**) which is based on Eq. 1.

Composition mapping in the SEM is useful way in dissociation various elements by identifying each element with a different color [17-19]. This technique makes a better understanding of elemental distribution in and around the microconstituents analyzed. Based on EDS spot scan results, the elements Ni, Cr, Si, Mo, Nb, C and Fe were chosen for analysis and are symbolized as the colors purple, green, yellow, cyan, light green, brown and dark green, respectively in **Fig. 9**. It shows a clear segregation of components corresponding to different phases in the micrograph of sample B. Fe depletion in these highly concentrated niobium regions gives a clear indication where Fe_2Nb particles exist, in confirmation with **Fig. 5** which indicated that the Laves phase particle is type of Fe_2Nb. In agreement with what has been reported by S.W. Chen et al [20].

DOI 10.12776/ams.v24i4.1160 p-ISSN 1335-1532
e-ISSN 1338-1156

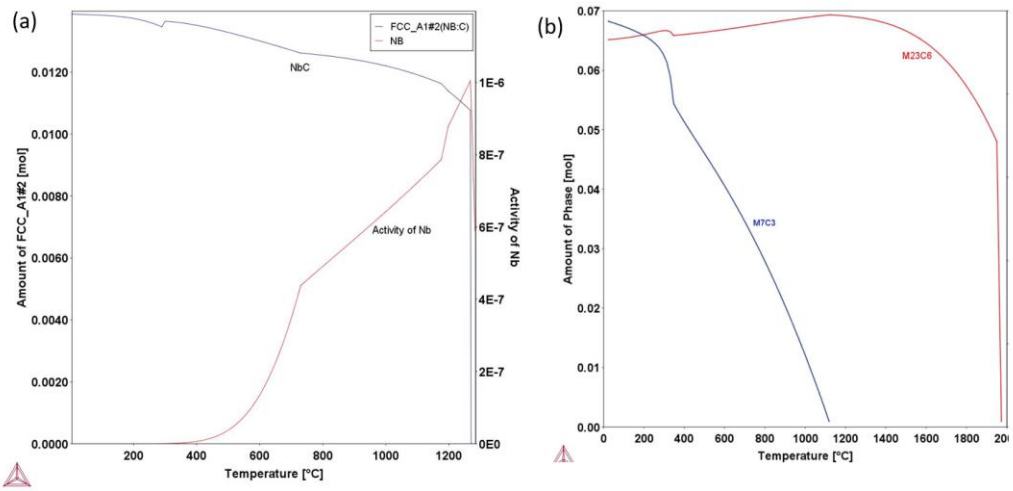

Fig. 8 Thermodynamic simulation results for a) NbC stability and activity of Nb, and b) the amount of $Cr_{23}C_6$ and Cr_7C_3 vs Temperature with Thermo-Calc

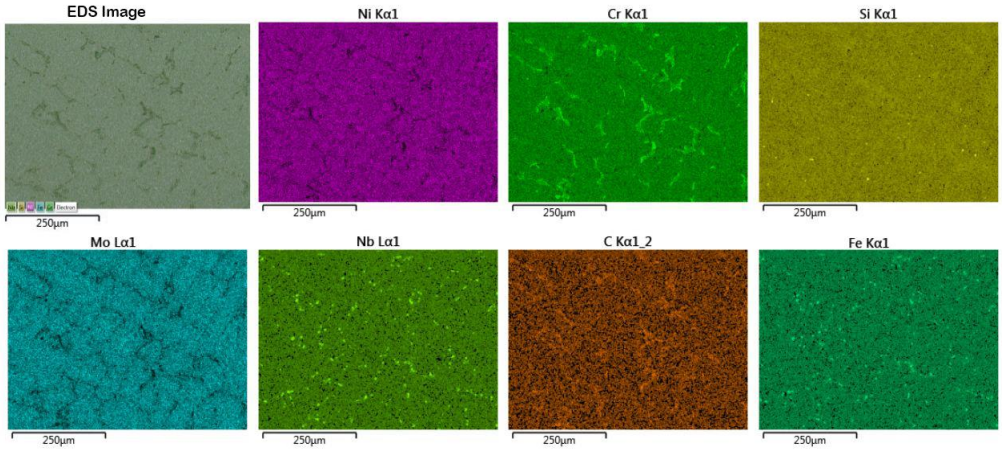

Fig. 9 Elemental distribution map of the sample after long term aging

4 Conclusion

The microstructure of two HP alloys (Fe-25Ni-35Cr) in two different conditions (as-cast and after 10 years' service at elevated temperature), from both the experimental and the modeling points of view has been studied. The main conclusions are the following:

1. The microstructure of as-cast alloy consists of an austenitic matrix containing several types of precipitates including NbC, Cr_7C_3 and Cr_3C and/or $Cr_{23}C_6$. Based on Scheil results, such structure is formed by crystallization under the influence of segregation of carbon and chromium and is a non-equilibrium one.
2. Aging at 900 °C for long-time results in the fragmentation of the primary structure of the eutectic carbides. At the same duration, secondary $Cr_{23}C_6$ carbide particles will

DOI 10.12776/ams.v24i4.1160 p-ISSN 1335-1532
e-ISSN 1338-1156

precipitate in intergranular regions and almost all Cr_7C_3 carbides transformed into $Cr_{23}C_6$ carbides. Moreover, some strong evidences related to formation of Laves phase during aging have been found.

3. Combination of EBSD-EDS technique with thermodynamic calculation is one of the novel and most accurate method to investigation of phase transformation, as the precipitations are identified on the basis of their crystal structure, chemical composition and their thermodynamic features.

Acknowledgements

The authors would you like to thank Hormozgan Steel Company for their support and collaboration during this project.

References

[1] M. Mostafaei, M. Shamanian, H. Purmohamad, M. Amini, A. Saatchi: ”Microstructural degradation of two cast heat resistant reformer tubes after long term service exposure”, Engineering Failure Analysis 18, 2011, p. 164–171

[2] A. Koblischka-Veneva, M. R. Koblischka, F. Mucklich: ”Advanced microstructural analysis of ferrite materials by means of electron backscatter diffraction (EBSD)”, Journal of Magnetism and Magnetic Materials, Vol. 322, 2010, p. 1178–1181

[3] J. Liu, D. Jiao, Ch. Luo: “Microstructural evolution in austenitic heat-resistant cast steel 35Cr25Ni12NNbRE during long-term service”, Materials Science and Engineering A, Vol. 527, 2010, P. 2772–2779

[4] V. Javaheri, F. Shahri, M. Mohammadnezhad, M. Tamizifar, M. Naseri: “The effect of Nb and Ti on structure and mechanical properties of 12Ni-25Cr-0.4C austenitic heat-resistant steel after aging at 900oC for 1000h”, Journal of Material Engineering and Performance, Vol. 23, 2014, p. 3558-3566

[5] B. Sonderegger, S. Mitsche, H. Cerjak, “Microstructural analysis on a creep resistant martensitic 9–12% Cr steel using the EBSD method”, Materials Science and Engineering A, Vol. 481–482, 2008, p. 466–470

[6] L.H.de Almeida, A.F. Ribeiro, I.L. May: ”Microstructural characterization of modified 25Cr–35Ni centrifugally cast steel furnace tubes”, Materials Characterization, Vol. 49, 2003, p. 219– 229

[7] P. Hilkhuijsen, H. J. M. Geijselaers, T. C. Bor: “The influence of austenite texture on the martensitic transformation of an austenitic stainless steel”, Journal of Alloys and Compounds, Vol. 577, 2013, p. 609–613

[8] J. Laigo, F. Tancret, R. L. Gall, J. Furtado: ”EBSD Phase Identification and Modeling of Precipitate Formation in HP Alloys”, Advanced Materials Research, Vol. 15-17, 2007, p. 702-707

[9] I. Aydin, H-E. Buehler, A. Rahmel: Precipitation in the heat resistant nickel-base cast alloys G-NiCr 28 W and G-NiCr 50 Nb. Arch Eisenhuettenwes, Vol. 54, 1983, p. 461–466

[10] E. Erdos: X-ray diffraction. In: Van der Biest O, editor, “Analysis of high temperature materials”, New York, Applied Science Publisher, 1983, p. 203–205

[11] S.Y. Kondrat'ev, V.S. Kraposhin, G.P. Anastasiadi, A.L. Talis: "Experimental observation and crystallographic description of M7C3 carbide transformation in Fe–Cr–Ni–C HP type alloy", Acta Materialia, Vol. 100, 2015, p. 275-281

[12] B. Sonderegger, S. Mitsche, H. Cerjak: "Martensite laths in creep resistant martensitic 9–12% Cr steels Calculation and measurement of misorientations", Materials Characterization, Vol. 58, 2007, p. 874–882

[13] B. Ravi Kumar, A. K. Singh, B. Mahato, P. K. De, N. R. Bandyopadhyay, D.K. Bhattachary: "Deformation-induced transformation textures in metastable austenitic stainless steel", Materials Science and Engineering A, Vol. 429, 2006, p. 205–211

[14] B. Peng, H. Zhang, J. Hong, J. Gao, H. Zhang, Q. Wang, J. Li: "The effect of M23C6 on the high-temperature tensile strength of two austenitic heat-resistant steels: 22Cr–25Ni–Mo–Nb–N and 25Cr–20Ni–Nb–N", Materials Science and Engineering A, Vol. 528, 2011, p. 3625–3629

[15] N. Nabiran, S. Klein, S. Weber, W. Theisen: "Evolution of the Laves Phase in Ferritic Heat-Resistant Steels during Long-term Annealing and its Influence on the High-Temperature Strength", Metallurgical and Materials Transaction A, Vol. 46A, 2015, p. 102-114

[16] J. Froitzheim, G. H. Meier, L. Niewolak, P. J. Ennis, H. Hattendorf, L. Singheiser, W.J. Quadakkers: "Development of high strength ferritic steel for interconnect application in SOFCs", Journal of Power Sources, Vol. 178, 2008, p. 163–173

[17] A. Wassilkowska , A. Czaplicka-kotas, M. Zielina, A. Bielski , "An analysis of the elemental composition of micro-samples using EDS technique ", Technical transactions ch-12 (2014) 133-148

[18] S. Burgess, L. Xiaobing, J. Holland: "High spatial resolution energy dispersive X-ray spectrometry in the SEM and the detection of light elements including lithium", Microscopy and Analysis, Vol. 6, 2013, p.. S8-S13

[19] BS ISO 22309. Microbeam analysis – Quantitative analysis using energy-dispersive spectrometry (EDS) for elements with an atomic number of 11 (Na) or above, 2011

[20] S. W. Chen, C. Zhang, Z. X. Xia, H. Ishikawa, Z. G. Yang: "Precipitation behavior of Fe2Nb Laves phase on grain boundaries in austenitic heat resistant steels", Materials Science & Engineering A, Vol. 616, 2014, p. 183–188

DOI 10.12776/ams.v24i4.1160 p-ISSN 1335-1532
e-ISSN 1338-1156